Oil Shale, 2018, Vol. 35, No. 3, pp. 230–241
doi: https://doi.org/10.3176/oil.2018.3.03
ISSN 0208-189X

CHANGES IN OIL SHALE CHARACTERISTICS DURING SIMULATED IN-SITU PYROLYSIS IN SUPERHEATED STEAM

LEI WANG, DONG YANG*, JING ZHAO, YANGSHENG ZHAO, ZHIQIN KANG

Institute of Mining Technology, Taiyuan University of Technology, Taiyuan 030024, P. R. China

Abstract. *Internal pores and fractures inside oil shale undergo complex changes during pyrolysis in superheated steam. After a simulated in-situ pyrolysis in superheated steam, the pore characteristics of 30 oil shale samples from different zones between the injection and production wells were investigated using mercury intrusion porosimetry (MIP). The results showed that the porosity of oil shale exceeded 27.65% in each position of horizontal fractures. In different types of pores, the proportions of mesopore (0.1 μm < d ≤ 1 μm) and micropore (d ≤ 0.015 μm) were the largest and the smallest, respectively. Moreover, mesopores outnumbered micropores. The pore structure of pyrolyzed oil shale after convection heating was complex. After the pyrolysis in superheated steam, the proportion of the oil shale ore body with a porosity ranging from 23 to 31% was 74.95% of total. This finding proved that oil shale was transformed from dense rock to a porous medium under the effect of superheated steam.*

Keywords: *superheated steam, mercury intrusion porosimetry, porosity, pore size distribution.*

1. Introduction

Oil shale is internationally recognized as an important alternative energy with huge reserves for oil and gas. China's oil shale reserves comprise approximately 354 billion barrels of shale oil, which accounts for 7% of its world reserves. The country has begun investing heavily in the study of the in-situ oil shale recovery technology to reduce its cost and improve mining efficiency.

The in-situ oil shale recovery requires hot injection wells to directly heat the ore body. Kerogen is cracked to produce shale oil and gas when oil shale

* Corresponding author: e-mail *ydscience@hotmail.com*

is fully pyrolyzed. In addition, oil and gas are discharged to the ground through production wells [1–4]. According to the form of heating, the in-situ recovery technology can be divided into heat conduction and convection heating. The inductively coupled plasma (ICP) technology of Shell uses electrodes in hot injection wells to elevate the temperature of oil shale. Oil shale is a tight sedimentary rock with poor thermal conductivity, and its temperature for in-situ recovery is above 265 °C after several years of thermal conduction [5]. The radio frequency technique of U.S. Lawrence Livermore National Laboratory (LLNL) uses very high radio frequencies to heat and decompose oil shale, making it easier to process [6–8].

Taiyuan University of Technology, China, proposed an in-situ technology for the recovery of oil shale in superheated steam. Superheated steam is used to heat oil shale to achieve high heating efficiency [9–12]. The university collected large oil shale samples from the Fushun West Open-pit Mine at the end of 2015. A laboratory test on large-size specimens was conducted to simulate the in-situ recovery of lump oil shale in superheated steam.

Earlier the effect of temperature on the yield of pyrolysis products and the change in the macro and micro characteristics of oil shale have been studied. In addition to temperature, the mode of heat transfer and crustal stress affect the pyrolysis characteristics of oil shale. However, no researcher has ever conducted studies on the effect of in-situ oil shale pyrolysis on its microscopic characteristics. Therefore, the investigation of the said effect during convection heating is important to evaluate the efficiency of in-situ recovery technology. Such an investigation would help establish the industrial in-situ recovery technology of oil shale in superheated steam.

2. Methods

Oil shale is a sedimentary rock with a distinct bedding structure. Factors such as composition and density affect the deformation of rock mass and the characteristics of fracture development. Fushun oil shale has a relatively high oil content, 15.02%, whereas that of other Chinese oil shales is 6–8% on average. The mineral composition of Fushun oil shale includes mainly quartz, kaolinite, calcite, illite, muscovite and pyrite. The X-ray diffraction (XRD) map of the oil shale is illustrated in Figure 1.

In a simulation experiment on the in-situ recovery of oil shale in superheated steam, cement, gangue and fine sand were mixed thoroughly and laid on the bottom of a 1700 mm × 1400 mm container. After drying, the large-size oil shale sample was placed in the container. The gap between the container and the oil shale was fully filled. When the filling material was entirely dry, a large iron plate with holes drilled earlier in it was placed on top of the container. Drilling holes were used for drilling and coring, the drilling depth was close to the bottom of the oil shale ore body. After the drilling was completed, tubes were pressed into drilling holes, and the gaps

between the tubes and the drillings holes were filled with temperature-resistant cement. Finally, the container was placed on a true three-axis pressure test machine, which can simulate the true pressure of oil shale formation. The temperature of superheated steam used for in-situ pyrolysis of oil shale was 550 °C. The oil shale ore body after the test is shown in Figure 2. The roof and underlying bedrocks depicted in the figure are both mixtures of cement, gangue and fine sand.

When pyrolysis of oil shale is carried out in superheated steam, many horizontal fractures are formed between the injection and production wells,

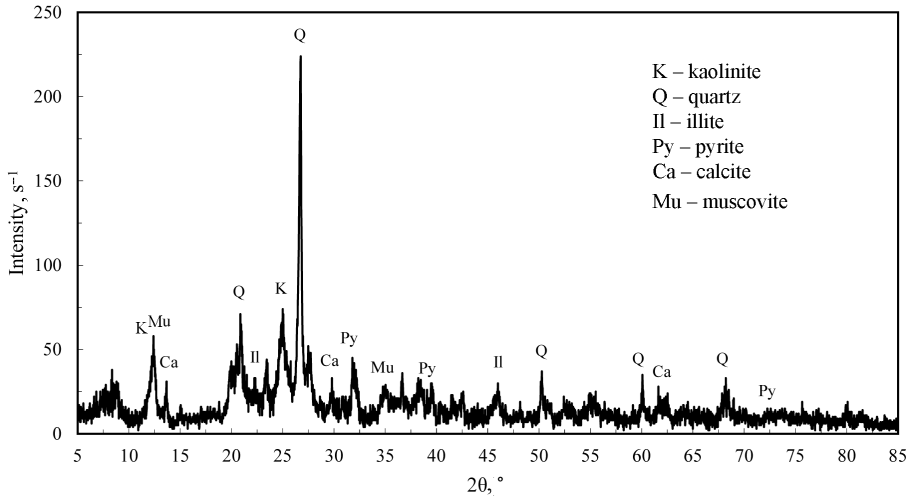

Fig. 1. XRD map of Fushun oil shale.

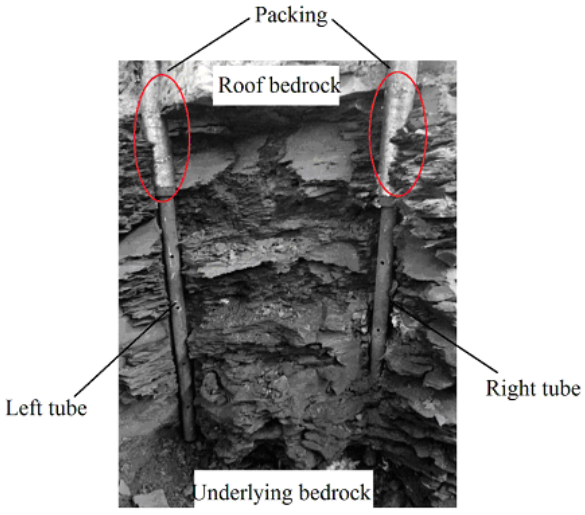

Fig. 2. The oil shale ore body after the test.

representing the main channels for steam pyrolysis. The authors sampled oil shale at different parts of the adjacent well tubes after completing the pyrolysis experiment. The sampling scheme will be discussed in the following section.

The oil shale thickness was 500 mm, and the spacing between adjacent well tubes was 300 mm. Five groups of 6 samples (i.e. altogether 30 samples, Fig. 3) were obtained from the underlying bedrock at 50, 150, 250, 350 and 450 mm. The horizontal spacing between every two samples was 60 mm. Three groups of samples from the underlying bedrock at 150, 250 and 350 mm were in the horizontal fracture direction. Therefore, the microscopic characteristics of oil shale in horizontal fractures could be obtained using its average porosity and permeability. The micro characteristics of the entire ore bed could be obtained through a statistical analysis of the porosity of all samples.

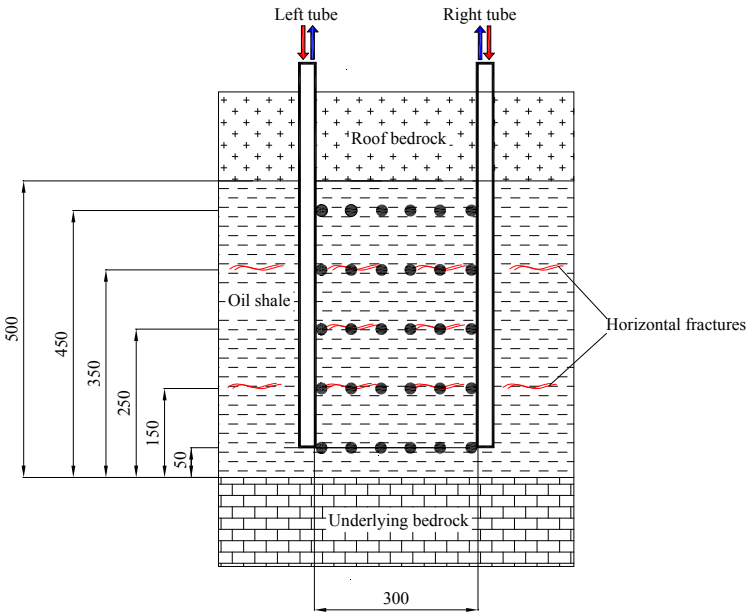

Fig. 3. Schematic of sampling points**.**

3. Results and discussion

3.1. Variation of the porosity and permeability of oil shale in horizontal fractures

The porosity and permeability of oil shale in different positions of horizontal fractures affect its interaction with superheated steam in the pyrolysis process. Figure 4 illustrates the variation of oil shale porosity and permeability in the horizontal cracks.

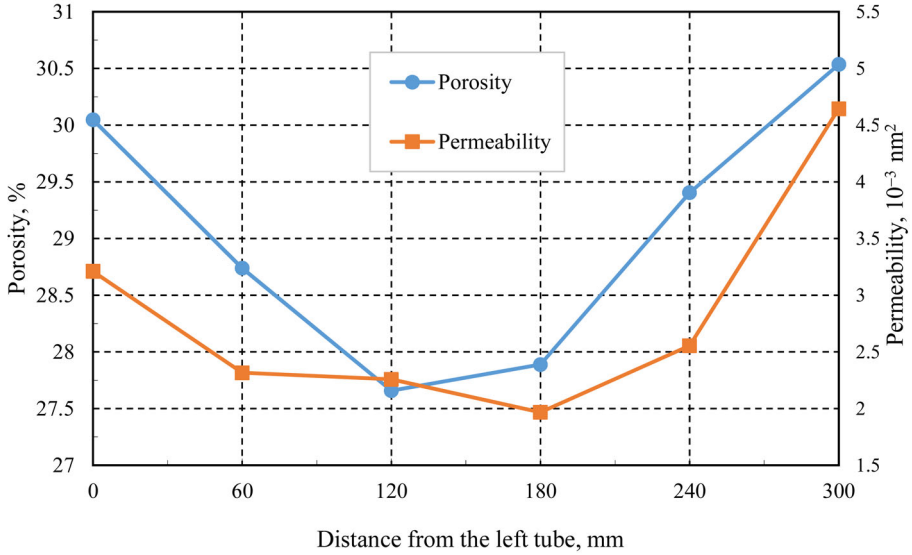

Fig. 4. Variation of the porosity and permeability of oil shale in the horizontal cracks.

Each tube can be used as a steam injection and oil production well in the simulated in-situ oil shale recovery in superheated steam. During the pyrolysis test, the right tube served as the injection well and the left tube served as the production well. After a few hours of the experiment, the left tube was used as the injection well and the right tube was employed as the production well for oil and gas exploration. From Figure 4 it can be seen that the porosity of oil shale in any position of the horizontal fractures was more than 27.65%. In the natural state, oil shale is a tight rock with a porosity of 3.94%, indicating that the porosity changes qualitatively during steam injection, which happens for the following reasons:

Firstly, during pyrolysis, organic matter in oil shale undergoes a phase transition from solid to liquid and then to gas, forming a considerable expansion stress in its pore space. This phenomenon causes rock damage and failure. The holes are formed in the rock mass after pyrolysis, and the porosity of oil shale increases further.

Secondly, carbonate and silicate minerals contained in oil shale are decomposed during low-temperature pyrolysis to a lesser degree, and the clay minerals undergo dehydration reactions in the temperature range of 400–550 °C in which the decomposition of illite ($K_2O \cdot Al_2O_3 \cdot 14SiO_2 \cdot 4H_2O$) and kaolinite ($2Al_2Si_2O_5 \cdot (OH)_4$) mainly occurs. The dehydration rate of kaolinite, which transforms into abundant metakaolin ($2Al_2Si_2O_7$), increases under the influence of high-pressure steam, as found by many researchers [13–15]. The related chemical reactions are as follows:

$$K_2O \cdot 5Al_2O_3 \cdot 14SiO_2 \cdot 4H_2O \rightarrow K_2O \cdot 5Al_2O_3 \cdot 14SiO_2 + 4H_2O, \quad (1)$$

$$2Al_2Si_2O_5 \cdot (OH)_4 \rightarrow 2Al_2Si_2O_7 + 4H_2O. \quad (2)$$

The porosity and permeability of oil shale in the intermediate position of the horizontal fractures are relatively low because the movement of steam and the pyrolysis of the ore body consume energy during convection heating by superheated steam. Consequently, the temperature and pressure of steam are low when it moves around the intermediate position of the fractures.

3.2. Pore distribution characteristics of oil shale in horizontal fractures

Figure 5 displays the variation in the porosity of pores of different sizes. According to the pore classification method used in mercury intrusion porosimetry (MIP), pores are divided into macropores ($d > 1$ μm), mesopores (0.1 μm $< d \leqslant 1$ μm), tiny pores (0.015 μm $< d \leqslant 0.1$ μm) and micropores ($d \leqslant 0.015$ μm). In any position of horizontal fractures, mesopores are dominant, followed by tiny pores, while macropores and micropores are the least developed pore types. However, the porosity of macropores is slightly higher than that of micropores. The porosity of pores decreases in the following order: mesopores > tiny pores > macropores > micropores.

Figure 5 shows that the porosity of macropores and micropores does not change much. On the one hand, oil shale not only undergoes complex chemical changes under the influence of superheated steam but also experiences physical changes revealed by thermal expansion. Such an expansion becomes apparent with the increase in heating temperature, but its

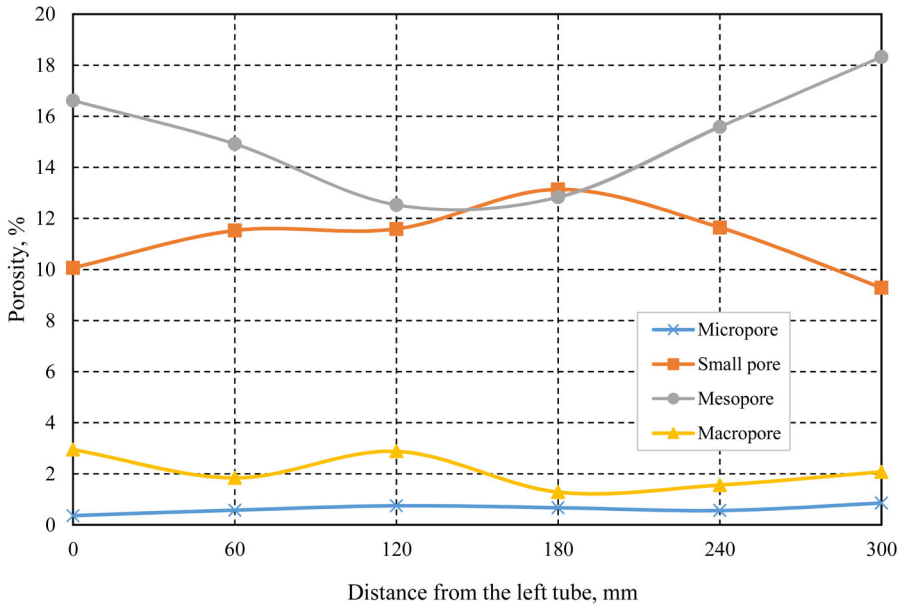

Fig. 5. Variation in the porosity of different sized pores in the horizontal fractures.

effect is restrained by the expansion of the interior space of oil shale. The porosity of macropores is low because the channels of hydrocarbon migration and the pores are compressed. On the other hand, in its natural state, fractures and pores in oil shale are but slightly developed from the viewpoint of rock mechanical characteristics. The internal deformation of oil shale at higher temperatures is quite chaotic, and a lot of energy is consumed for convection heating with superheated steam, which leads to the stratification of oil shale. Thus, the strength of oil shale is significantly reduced and plasticity is enhanced [16, 17]. Multiple macroscopic and microscopic deformations can easily occur under the combined action of high-pressure steam and external stress.

In horizontal fractures, the change of the porosity of mesopores is opposite to that of tiny pores. The production of oil and gas by kerogen pyrolysis increases the size of pores when the steam temperature is high, as a result, tiny pores become mesopores. Certain kerogens decompose to produce shale oil and gas when the steam temperature is relatively low, while other kerogens are converted into asphaltene, which blocks the pores. Therefore, the porosity of mesopores decreases while that of tiny pores increases.

3.3. Pore structure characteristics of oil shale during pyrolysis

In the simulated in-situ recovery of oil shale in superheated steam, most of the oil shale is pyrolyzed by convection heating, whereas the oil shale near the roof bedrock section is pyrolyzed through heat conduction. However, the efficiency of heat conduction is low. From Figures 6(a)–(c) it can be seen that the shapes of mercury injection and withdrawal curves of different oil shale samples are different.

The mercury injection/withdrawal curves of oil shale convection heating are displayed in Figure 6(a). The mercury injection curve has an S shape. The smooth withdrawal curve demonstrates apparent hysteresis at the beginning of the withdrawal stage. The internal pore structure of oil shale is complicated, and a minimal amount of mercury is retained in the bottleneck pores. The mercury withdrawal curve decreases gradually, and the removal efficiency is significant.

The mercury injection/withdrawal curves of oil shale pyrolyzed by heat conduction are depicted in Figures 6(b)–(c). From Figure 6(b) it can be seen that the mercury injection curve has an inversed-S shape, and it is nearly parallel to the mercury withdrawal curve. Hysteresis is not observed and practically no mercury remains in the bottleneck pores. Figure 6(c) shows that the mercury injection curve is of the inversed-S shape as well, and the mercury withdrawal curve is nearly parallel to the coordinate axis. Almost no withdrawal of mercury is observed. Overall, the volume of mercury injected remains unchanged with pore size changing from 100 to 100,000 mm. The pores in this size range are virtually undeveloped. Therefore, the pore structure of oil shale pyrolyzed through heat conduction is relatively simple.

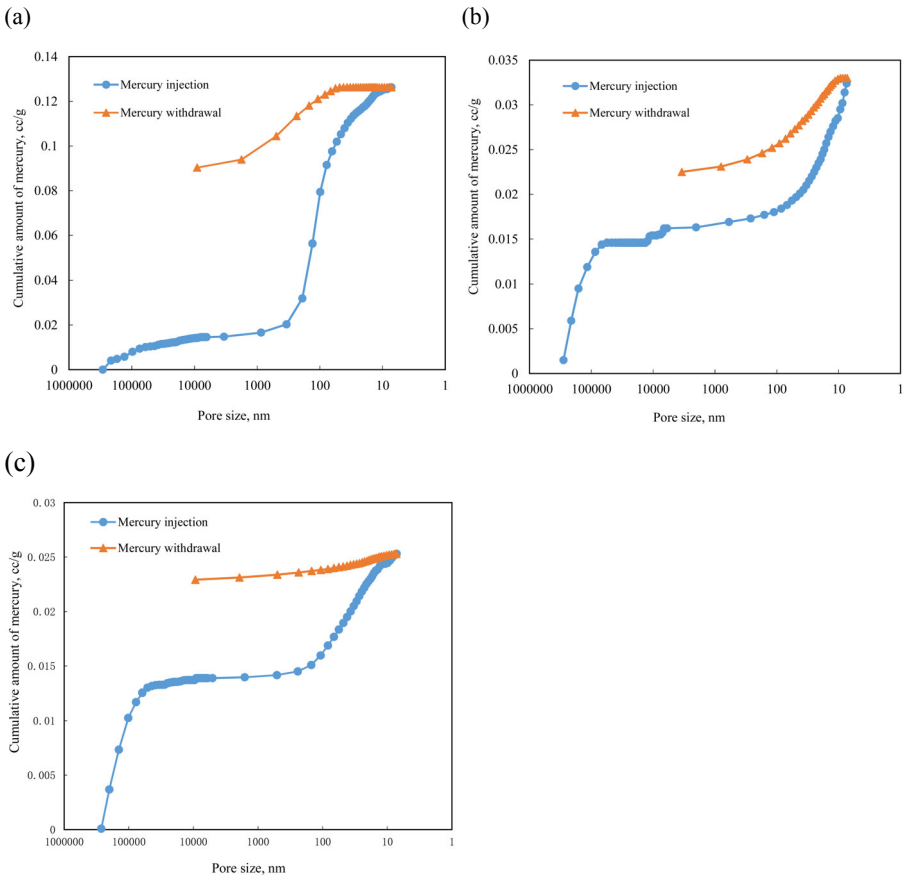

Fig. 6. Mercury injection and withdrawal curves of oil shale by (a) convection heating, (b)–(c) heat conduction.

3.4. Porosity distribution characteristics of oil shale during pyrolysis

The porosity of oil shale at different positions between the left and right tubes is statistically analyzed and plotted using the Origin software, and the distribution of oil shale porosity during the entire pyrolysis process is obtained (Fig. 7).

The porosity of oil shale near the roof bedrock section is low, mostly less than 5%, indicating that the heating efficiency of heat conduction is extremely low and Fushun oil shale is a tight rock. However, the porosity of the entire oil shale ore body is mostly higher, which is indicative of the efficiency of convection heating. The porosity nephogram of oil shale is asymmetric in the horizontal and vertical directions, suggesting that oil shale is apparently anisotropic and the bedding structure is obvious. The interlayer is filled with several low-strength argillaceous minerals. Therefore, the strength of the interlayer is low and it is easily ruptured under steam

pressure. The range of pyrolysis that corresponds to oil shale samples of different porosities is quantitatively analyzed, as depicted in Figure 8.

The pyrolysis range of oil shale is the widest when its porosity is between 29 and 31%, accounting for 30.31% of the entire pyrolysis area. The pyrolysis range of oil shale is the smallest when the porosity is between 5 and 7%, which represents 1.31% of the entire pyrolysis area. Overall, the

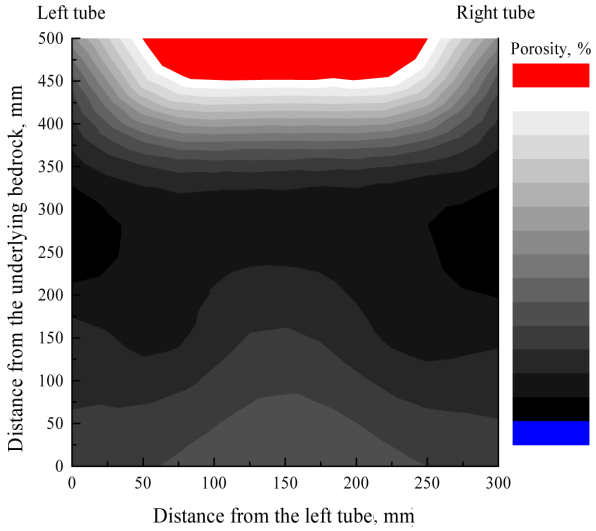

Fig. 7. Nephogram of the porosity distribution of oil shale.

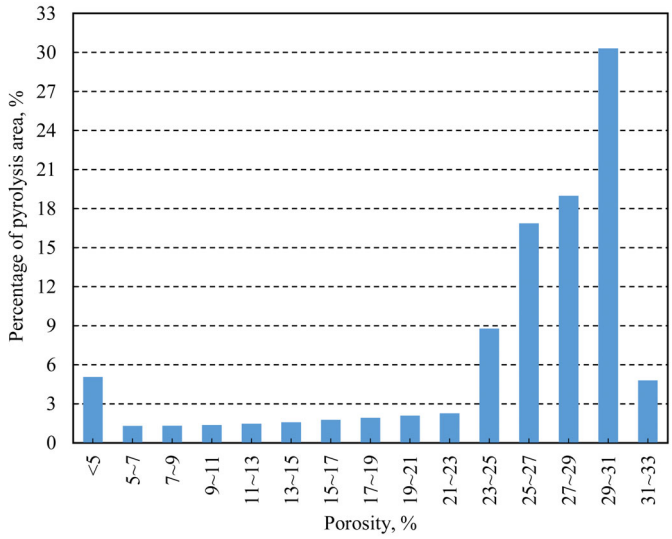

Fig. 8. Histogram of the percentage of pyrolysis zone corresponding to oil shale samples of various porosities.

porosity of the ore body is between 23 and 31%, accounting for 74.95% of the total area of pyrolysis. This is attributed to the high temperature and pressure of superheated steam, as well as the weakly cementing surface inside oil shale, which is easily ruptured under thermal stress and high steam pressure. The ruptured surfaces are then connected to one another to form a large-scale mesh structure, which expands the area of heat exchange and allows high-temperature steam as a carrier of heat to pyrolyze oil shale faster.

It has been reported in the literature that the organic matter in Fushun oil shale can be fully pyrolyzed at a critical temperature of 500 °C [18, 19]. The porosity of oil shale at this temperature increases abruptly by more than 20%. Thus, the degree of oil shale porosity can indicate the extent of pyrolysis of an ore bed. Based on this, the authors believe that oil shale undergoes no pyrolysis when its porosity is below 5%. The pyrolysis degree of oil shale is low when its porosity is 5–19%, and very high when the porosity is more than 20%. Therefore, the percentage of the non-pyrolyzed oil shale ore bed is only 5.06%, that of the incompletely pyrolyzed ore bed is 10.74%, and of the fully pyrolyzed ore bed 84.2%.

4. Conclusions

The in-situ recovery technology of oil shale in superheated steam utilizes high temperature and high pressure for its pyrolysis. A simulated in-situ oil shale pyrolysis test in superheated steam is conducted. After the test, the porosity, permeability and pore characteristics of oil shale samples from various zones between the injection and production wells are tested through mercury intrusion porosimetry. The main conclusions are as follows:

1. The porosity of oil shale in each position of horizontal fractures is more than 27.65%, indicating that it changes qualitatively under steam injection. The porosity and permeability of oil shale in the intermediate position of horizontal fractures are relatively low.
2. In any position of horizontal fractures, the porosity of pores decreases in the following order: mesopores > tiny pores > macropores > micropores. Among the pores, mesopores dominate.
3. The pore structure of oil shale pyrolyzed by convection heating is complex, whereas that of oil shale pyrolyzed through heat conduction is relatively simple. The porosity of the pyrolyzed oil shale ore bed is between 23 and 31%. The percentage of the non-pyrolyzed oil shale ore bed is only 5.06%, and that of the fully pyrolyzed ore bed reaches 84.2%.
4. A theoretical basis for developing the in-situ recovery technology of oil shale in superheated steam is created by studying the microscopic characteristics of Fushun oil shale after simulated in-situ pyrolysis, which provides a reference for the design of the oil shale recovery process in superheated steam.

Acknowledgments

This work was supported by the National Natural Science Foundation of China (Nos. U1261102, 51704206), and the Innovative Graduate Education Project of Shanxi Province, China (No. 2016SY013).

REFERENCES

1. Liu, R., Liu, Z. J. Oil shale resource situation and multi-purpose development potential in China and abroad. *Journal of Jilin University (Earth Science Edition)*, 2006, **36**(6), 892–898 (in Chinese).
2. Zhao, J., Yang, D., Kang, Z. Q., Feng, Z. C. A Micro-Ct study of changes in the internal structure of Daqing and Yan'an oil shales at high temperatures. *Oil Shale*, 2012, **29**(4), 357–367.
3. Liu, Z. J., Dong, Q. S., Ye, S. Q., Zhu, J. W., Guo, W., Li, D. C., Liu, R., Zhang, H. L., Du, J. F. The situation of oil shale resources in China. *Journal of Jilin University (Earth Science Edition)*, 2006, **36**(6), 869 – 876 (in Chinese).
4. Hao, Y., Gao, X. Q., Xiong, F. S., Zhang, J. L., Li, Y. J. Temperature distribution simulation and optimization design of electric heater for in-situ oil shale heating. *Oil Shale*, 2014, **31**(2), 105–120.
5. Han, H., Zhong, N. N., Huang, C. X., Liu, Y., Luo, Q. Y., Dai, N., Huang, X. Y. Numerical simulation of in situ conversion of continental oil shale in Northeast China. *Oil Shale*, 2016, **33**(1), 45–57.
6. Yu, X. D., Luo, Z. F., Yang, X. L., Jiang, H. S., Zhou, E. H., Zhang, B., Dong, L. Oil shale separation using a novel combined dry beneficiation process. *Fuel*, 2016, **180**, 148–156.
7. Burnham, A. K., Mcconaghy, J. R. Comparison of the acceptability of various oil shale processes. *26th Oil Shale Symposium, Colorado School of Mines, 16–19 October 2006,* Colorado, USA.
8. Bai, F. T. Theoretical and experimental research of oil shale pyrolysis triggered by topochemical heat. PhD Thesis, Changchun: Jilin University, 2015 (in Chinese).
9. Dyni, J. R. Geology and resources of some world oil-shale deposits. *Oil Shale*, 2003, **20**(3), 193–252.
10. Kang, Z. Q., Zhao, Y. S., Yang, D. Physical principle and numerical analysis of oil shale development using in-situ conversion process technology. *Acta Petrolei Sinica*, 2008, **29**(4), 592–595 (in Chinese).
11. Kang, Z. Q., Yang, D., Zhao, Y. S., Hu, Y. Q. Thermal cracking and corresponding permeability of Fushun oil shale. *Oil Shale*, 2011, **28**(2), 273–283.
12. Yang, L. S., Yang, D., Zhao, J., Liu, Z. H., Kang, Z. Q. Changes of oil shale pore structure and permeability at different temperatures. *Oil Shale*, 2016, **33**(2), 101–110.
13. Cao, D. G., Su, D. G., Yang, Z. Y., Song, G. S. Study of the microstructure of metakaolinite with IR, TG, SEM, XRD methods. *Acta Mineralogica Sinica*, 2004, **24**(4), 366–372 (in Chinese).
14. Bhargava, S., Awaja, F., Subasinghe, N. D. Characterisation of some Australian oil shale using thermal, X-ray and IR techniques. *Fuel*, 2005, **84**(6), 707–715.
15. Liu, W., Muhammad, N., Chen, J., Spiers, C. J., Peach, C. J., Deyi, J., Li, Y. P. Investigation on the permeability characteristics of bedded salt rocks and the

tightness of natural gas caverns in such formations. *Journal of Natural Gas Science & Engineering*, 2016, **35**, 468–482.
16. Li, Q. Simulation of temperature field and experiment of in-situ oil shale pyrolysis. PhD Thesis, Changchun: Jilin University, 2012 (in Chinese).
17. Li, Z. Q., Xian, X. F., Long, Q. M. Experiment study of coal permeability under different temperatures and stresses. *Journal of China University of Mining & Technology*, 2009, **38**(4), 523–527 (in Chinese).
18. Yang, D., Kang, Z. Q., Zhao, J., Zhao, Y. S. CT Experiment research of oil shale under high temperature. *Journal of Taiyuan University of Technology*, 2011, **42**(3), 255–257 (in Chinese).
19. Bai, F. T., Sun, Y. H., Liu, Y. M., Guo, M. Y. Evaluation of the porous structure of Huadian oil shale during pyrolysis using multiple approaches. *Fuel*, 2017, **187**, 1–8.

Presented by I. Aarna
Received September 9, 2017